Synthesis crystal structure and magnetic properties of [Fe2(bpym)(C5O5)2(H2O)4]·2H2O and two polymorphs of [Fe2(bpym)(C4O4)2(H2O)6]·2H2O (bpym = 2,2′-bipyrimidine)

Article *in* Inorganica Chimica Acta · October 1998

DOI: 10.1016/S0020-1693(98)00038-3

CITATIONS
38

READS
32

4 authors, including:

Harbi Daraghmeh
Arab American University
4 PUBLICATIONS **46** CITATIONS

SEE PROFILE

Miguel Julve
University of Valencia
684 PUBLICATIONS **26,504** CITATIONS

SEE PROFILE

ELSEVIER

Inorganica Chimica Acta 279 (1998) 127–135

Inorganica Chimica Acta

Synthesis, crystal structure and magnetic properties of $[Fe_2(bpym)(C_5O_5)_2(H_2O)_4]\cdot 2H_2O$ and two polymorphs of $[Fe_2(bpym)(C_4O_4)_2(H_2O)_6]\cdot 2H_2O$ (bpym = 2,2′-bipyrimidine)

Jorunn Sletten [a,*], Harbi Daraghmeh [a], Francesc Lloret [b], Miguel Julve [b]

[a] *Department of Chemistry, University of Bergen, 5007 Bergen, Norway*

[b] *Departament de Química Inorgànica, Facultat de Química de la Universitat de València, Dr. Moliner 50, 46100 Burjassot València, Spain*

Received 29 October 1997; received in revised form 12 December 1997; accepted 12 January 1998

Abstract

Two dinuclear iron(II) complexes of formulae $[Fe_2(bpym)(C_5O_5)_2(H_2O)_4]\cdot 2H_2O$ (**1**) and $[Fe_2(bpym)(C_4O_4)_2(H_2O)_6]\cdot 2H_2O$ (**2**) (bpym = 2,2-bipyrimidine, $C_5O_5^{2-}$ = dianion of croconic acid (4,5-dihydroxycyclopent-4-ene-1,2,3-trione) and $C_4O_4^{2-}$ = dianion of squaric acid (3,4-dihydroxycyclobut-3-ene-1,2-dione)) were prepared and their crystal structures (at 103 K) determined by X-ray diffraction methods. The structure of **1** consists of neutral centrosymmetric $[Fe_2(bpym)(C_5O_5)_2(H_2O)_4]$ units and water molecules of crystallization which are linked by an extensive network of hydrogen bonds. The coordination geometry around each iron atom is that of a compressed octahedron with bpym nitrogen atoms and croconate oxygen atoms in the equatorial positio..., .nd water molecules in the axial positions. The croconate and bpym ligands adopt bidentate and bisbidentate coordination modes respectively. Compound **2** exhibits two different polymorphic forms, denoted **2i** and **2ii**. The two molecular structures are made up of neutral centrosymmetric $[Fe_2(bpym)(C_4O_4)_2(H_2O)_6]$ units and water of hydration, the main difference between the two forms being in the packing and hydrogen bond pattern. Each iron atom has a highly distorted octahedral geometry with bpym nitrogen atoms, one squarate oxygen and a water molecule in equatorial positions, and water molecules in axial positions. Squarate and bpym ligands adopt monodentate and bisbidentate coordination modes respectively. The intradimer metal–metal separations are 5.829(2) (**1**), 5.869(1) (**2i**) and 5.941(3) Å (**2ii**). The magnetic behaviour of **1** and **2i** in the temperature range 290–2 K is characteristic of an intradimer antiferromagnetic coupling, the susceptibility curves exhibiting maxima at 11.5 (**1**) and 18.5 K (**2i**). A magnetostructural comparison with other bpym-bridged iron(II) complexes is carried out.

Keywords: Crystal structures; Magnetic properties; Iron complexes; Croconate complexes; Squarate complexes

1. Introduction

Although the first preparations of the monocyclic oxocarbon dianions squarate (dianion of 3,4-dihydroxycyclobut-3-ene-1,2-dione, $H_2C_4O_4$) and croconate (dianion of 4,5-dihydroxycyclopent-4-ene-1,2,3-trione, $H_2C_5O_5$) date from 1821 [1] and 1959 [2], their coordination chemistry has been the subject of current research activity in the last two decades [3–17]. It deserves to be noted that a successful general method for the synthesis of the so-called aromatic oxocarbon dianions, $C_nO_n^{2-}$ (n = 3–6), which uses di-tert-butoxyethyne as starting product, was proposed only in 1983 [18]. The fact that squaric acid is a stable and commercially available product, and the knowledge of simple but efficient methods of synthesis of stable croconate salts using either MnO_2 [19] or H_2O_2 [20] as the oxidant agent towards rhodizonate (5,6-dihydroxycyclohex-5-ene-1,2,3,4-tetronate), opened new perspectives to coordination chemists. Both ligands react with divalent transition metal ions to yield chain compounds of formula $[M(C_4O_4)(H_2O)_4]$ [10b] and $[M(C_5O_5)(H_2O)_3]$ [15a,c,17a] where the metal ions are bridged by squarate or croconate, the former acting as a 1,3-bis(monodentate) ligand and the latter adopting simultaneously monodentate and bidentate coordination modes. Curiously, the squarate exhibits a tetrakismonodentate coordination mode in the compounds of formula $[M(C_4O_4)(H_2O)_2]$ (M = Mn, Fe, Co, Ni and Zn) leading to a sheetlike structure [11a]. The use of chelating ligands precludes the formation of these insoluble polymers and allows the preparation of nuclearity tailored complexes [10a,11e,12b–h,15b,17b–f].

* Corresponding author. Tel.: +47-5558 3562; fax: +47-5558 9490; e-mail: jorunn.sletten@kj.uib.no

0020-1693/98/$ - see front matter
PII S0020-1693(98)00038-3

The present work is devoted to analysis of the blocking role of a bischelating ligand such as 2,2′-bipyrimidine (bpym), aiming at precluding the formation of the corresponding squarate [10b] and croconate [15c] iron(II) chains and designing discrete polynuclear species. We present here the preparation and the structural and magnetic characterization of two dinuclear iron(II) complexes of formulae $[Fe_2(bpym)(C_5O_5)_2(H_2O)_4]\cdot 2H_2O$ (**1**) and $[Fe_2(bpym)(C_4O_4)_2(H_2O)_6]\cdot 2H_2O$ (**2**).

2. Experimental

2.1. Materials

2,2′-Bipyrimidine, squaric acid and anhydrous iron(II) chloride were Alfa, Aldrich and Fluka chemicals and were used as received. Potassium croconate was synthesized according to the literature [19,20].

2.2. Preparation of compounds

2.2.1. $[Fe_2(bpym)(C_5O_5)_2(H_2O)_4]\cdot 2H_2O$ (1)

1 mmol of $FeCl_2$ was dissolved in water (50 ml) together with 2 mmol of bpym. To the resulting dark red solution an aqueous solution containing 1 mmol of $K_2C_5O_5$ was added dropwise under constant stirring. The reddish brown solution was filtered and left at room temperature for slow evaporation. Irregularly shaped, brown crystals appeared after 1 day. They were collected by filtration, washed with diethyl ether and dried on filter paper in the open air. X-ray crystallographic structure determination (see below) proved the identity of this compound **1**. Evaporation of the remaining solution leads to yellow needles of $K_2C_5O_5$ and to hexagonal red plates of formula $[Fe(bpym)_3]Cl_2\cdot 7H_2O$ (**3**). The latter complex is a low-spin species which is already known [21]. The structure of the corresponding perchlorate salt has been reported very recently [22].

2.2.2. $[Fe_2(bpym)(C_4O_4)_2(H_2O)_6]\cdot 2H_2O$ (2)

1 mmol of $FeCl_2$ was dissolved in water (50 ml) together with 2 mmol of bpym. To the resulting dark red solution an aqueous solution containing 1 mmol of $Li_2C_4O_4$ (prepared in situ by mixing stoichiometric amounts of $H_2C_4O_4$ and $LiOH\cdot H_2O$) was added dropwise under constant stirring. The reddish brown solution was filtered and left at room temperature for slow evaporation. Brown crystals appeared after 1 day. The crystals were collected by filtration, washed with diethyl ether and dried on filter paper in open air. Optical inspection indicated that two different types of crystals, truncated pyramids and thin parallelepipeds, were present. X-ray crystallographic structure determinations (see below) showed that these were two different polymorphic forms of compound **2**, formula $[Fe_2(bpym)(sq)_2(H_2O)_6]\cdot 2H_2O$, hereafter noted **2i** and **2ii**. After collection of the first crop of brown crystals, the filtrate was left for further evaporation. After a few days thin, red, needle shaped crystals appeared (compound **4**). The chemical analysis (C, 36.76; H, 3.64; N, 15.49; Fe, 12.3; Cl, negative (%)) points towards an impure compound containing a 2:3:2 iron:bpym:squarate molar ratio. Further evaporation of the filtrate, to almost complete dryness, yielded the same red, hexagonal plates as observed in the previous synthesis (**3**). Compound **3** was later synthesized directly by mixing aqueous solutions of $FeCl_2$ and bpym in a molar ratio 1:3. Crystals of the latter two products, **3** and **4**, were not of X-ray quality.

2.3. Physical measurements

IR spectra were recorded on a Nicolet Impact 410 spectrophotometer as KBr pellets in the 4000–400 cm^{-1} region. Electronic spectra in DMSO (**1**, **2** and **4**) and aqueous (**3** and **4**) solutions were recorded (200–900 nm) using a Varian Cary 1 spectrophotometer. ^1H and ^{13}C NMR spectra were recorded with a Bruker 200 MHz instrument. The variable temperature magnetic susceptibility measurements were carried out on polycrystalline samples of **1** and **2i** in a field of 0.1 T using a Quantum Design SQUID magnetometer. The susceptometer was calibrated with $(NH_4)_2Mn(SO_4)_2\cdot 12H_2O$.

2.4. Crystal structure determinations and refinements

The crystals were sealed and mounted in paraton-n oil. Diffraction data were in each case collected with an Enraf-Nonius CAD-4 diffractometer equipped with a liquid-nitrogen cooling device, using graphite-monochromated Mo Kα radiation. Data collection conditions, crystal parameters and refinement results are summarized in Table 1. Cell dimensions were determined based on setting angles of 25 reflections in the 2θ ranges 28–38° (**1**), 30–41° (**2i**) and 30–38° (**2ii**). Intensity data were recorded using the $\omega/2\theta$ scan technique. Three reference reflections monitored throughout each data collection showed no significant decay for **1** and **2i**; for **2ii** there was a slight decay of 2.2% on average. The data were corrected for Lorentz polarization effects and for linear decay (**2ii**). For compound **2ii** the intensity profiles were unsymmetric and pronounced splitting of reflections was observed. Room temperature data collection was attempted to avoid cracking, but the extremely thin crystals then disintegrated quickly in the X-ray beam. Absorption corrections based on ψ-scan measurements were carried out for **1** and **2i** using 5 and 6 reflections respectively [23]. The structures were solved in space group $P\bar{1}$ (space group chosen based on intensity distributions) by the Patterson method (**1** and **2ii**) and by direct methods (**2i**), and refined by full-matrix least-squares. For compounds **1** and **2i** non-hydrogen atoms were refined anisotropically. Hydrogen atoms bonded to carbon were included at idealized calculated positions. Hydrogen atoms bonded to oxygen atoms were located in difference Fourier maps and were refined isotropically. For compound

Table 1
Summary of crystal data and structure refinement for $[Fe_2(bpym)(C_5O_5)_2(H_2O)_4]\cdot 2H_2O$ (**1**), $[Fe_2(bpym)(C_4O_4)_2(H_2O)_6]\cdot 2H_2O$ (**2**) polymorphs i and ii

Compound	1	2i	2ii
Empirical formula	$C_{18}H_{18}Fe_2N_4O_{16}$	$C_{16}H_{22}Fe_2N_4O_{16}$	$C_{16}H_{22}Fe_2N_4O_{16}$
Formula weight (g mol^{-1})	658.06	638.08	638.08
Temperature (K)	103(2)	103(2)	103(2)
Wavelength (Å)	0.71073	0.71073	0.71073
Space group	$P\bar{1}$	$P\bar{1}$	$P\bar{1}$
a (Å)	6.798(2)	7.312(1)	7.618(2)
b (Å)	9.231(3)	8.111(2)	8.595(4)
c (Å)	9.377(3)	9.989(2)	10.211(5)
α (°)	89.09(3)	84.99(2)	67.61(3)
β (°)	77.83(3)	81.75(1)	76.87(3)
γ (°)	89.25(2)	78.85(1)	75.63(3)
V (Å^3)	575.1(3)	574.1(2)	592.2(5)
Z	1	1	1
ρ_{calc} (g cm^{-3})	1.900	1.845	1.789
μ (mm^{-1})	1.356	1.354	1.308
$F(000)$	334	326	326
Crystal size (mm)	0.14×0.11×0.04	0.17×0.12×0.10	0.25×0.09×0.01
Max. 2θ (°)	50	50	50
Independent reflections	2000	2008	2054
Data, restraints, parameters	1998, 0, 205	2008, 0, 184	1651, 0, 77
Reflections with $I>2\sigma(I)$	1873	1900	1651
$R1$ ($I>2\sigma(I)$)	0.0292	0.0453	0.0887
$wR2$ ($I>2\sigma(I)$)	0.0741	0.1211	
Goodness of fit S on F^2	1.135	1.045	2.884

$R1=\Sigma||F_o|-|F_c||/\Sigma|F_o|$; $wR2=\{\Sigma[w(F_o^2-F_c^2)^2]/\Sigma[w(F_o^2)^2]\}^{1/2}$; $S=\{\Sigma[w(F_o^2-F_c^2)^2]/(n-p)\}^{1/2}$. For **1** and **2i** $w=1/\sigma^2(F_o^2)+(aP)^2+bP$, where a is 0.0339 (**1**) and 0.0916 (**2i**), b is 0.7567 (**1**) and 0.4699 (**2i**), $P=[0.3333(\text{maximum of 0 or } F_o^2)+0.6667F_c^2]$. For **2ii** $w=1$. For compounds **1** and **2i** refinement has been performed on F^2 including all reflections, for compound **2ii** refinement on F has been used, including reflections with $I>2\sigma(I)$.

2ii the experimental ψ-scan absorption correction was not adequate; instead a Fourier series empirical absorption correction [24] was done after isotropic refinement of all non-hydrogen atoms. Because of the type of absorption correction used, the final refinement was also isotropic. Hydrogen atoms bonded to carbon were included at idealized calculated positions, while hydrogen atoms bonded to water oxygen atoms were not included as they could not be located from Fourier difference maps. For compound **2ii** refinement in space group $P1$ was attempted, but was not successful. Refinements of **1** and **2i** were based on F^2 and included all reflections. For compound **2ii** the refinement was based on F, including reflections with $I>2\sigma(I)$; furthermore, 20 reflections with very uneven background were omitted from the calculations. The refinements converged at conventional R-values of 0.0292 (**1**), 0.0453 (**2i**) and 0.0887 (**2ii**); in all cases the values refer to reflections with $I>2\sigma(I)$.

For compounds **1** and **2i** the data reduction and absorption correction were performed with the Blessing programs [25], and all other calculations with the SHELXS-86, SHELXL-93 and XPL programs [26]. For compound **2ii** the MolEN program system [27] was used, in order to allow the Fourier series type absorption correction. Selected bond distances and angles and hydrogen bond parameters are given in Tables 2–7.

3. Results and discussion

3.1. IR and NMR spectra

The IR spectra of **1** and **2i** + **2ii** are dominated by a strong and broad band centred at around 1510 cm^{-1}, which is characteristic of salts of the $C_nO_n^{2-}$ ($n=4$–6) ions and is attributed to vibrational modes representing mixtures of C–O and C–C stretching motions [28]. Weak bands at 1796 and 1790 cm^{-1}, respectively, are associated with stretching vibrations of non-coordinated C=O bonds [29]. The IR spectrum of compound **4** is again dominated by a broad band centred around 1500 cm^{-1}, showing the presence of squarate in this compound. This feature obscures the ring stretching modes of bpym, and precludes the use of this region to identify the coordination mode of bpym [30]. A single sharp peak in the 1200–1250 cm^{-1} region has also been used to identify the bis(chelating) coordination mode of bpym [17f], however, in the present case the features in this region are weak and broad and do not give any conclusive evidence. In compound **3** two sharp peaks at 1573 and 1560 cm^{-1} show the presence of chelating, terminal bpym [30], and show that no squarate is present. These features of the IR spectrum of compound **3** are similar to those observed for $[Fe(bpym)_3](ClO_4)_2\cdot 1/4H_2O$ [22].

Table 2
Selected bond lengths (Å) and angles (°) for $[Fe_2(bpym)(C_5O_5)_2(H_2O)_4]\cdot 2H_2O$ (1)

Iron coordination sphere			
Fe–O(7)	2.025(2)	Fe–N(1)	2.186(2)
Fe–O(6)	2.084(2)	Fe–N(2)'	2.201(2)
Fe–O(5)	2.157(2)	Fe–O(1)	2.215(2)
O(7)–Fe–O(6)	176.67(7)	O(5)–Fe–N(2)'	170.50(7)
O(7)–Fe–O(5)	87.35(7)	N(1)–Fe–N(2)'	76.11(7)
O(6)–Fe–O(5)	95.31(7)	O(7)–Fe–O(1)	90.46(8)
O(7)–Fe–N(1)	91.63(8)	O(6)–Fe–O(1)	88.02(7)
O(6)–Fe–N(1)	90.11(7)	O(5)–Fe–O(1)	80.31(6)
O(5)–Fe–N(1)	95.59(7)	N(1)–Fe–O(1)	175.31(7)
O(7)–Fe–N(2)'	88.28(8)	N(2)a–Fe–O(1)	108.15(7)
O(6)–Fe–N(2)'	89.38(7)		
Croconate group			
O(1)–C(5)	1.265(3)	C(5)–C(9)	1.449(3)
O(2)–C(6)	1.244(3)	C(5)–C(6)	1.456(3)
O(3)–C(7)	1.236(3)	C(6)–C(7)	1.477(3)
O(4)–C(8)	1.239(3)	C(7)–C(8)	1.484(3)
O(5)–C(9)	1.262(3)	C(8)–C(9)	1.466(3)
C(5)–O(1)–Fe	105.90(14)	O(3)–C(7)–C(8)	127.1(2)
C(9)–O(5)–Fe	107.8(2)	C(6)–C(7)–C(8)	108.7(2)
O(1)–C(5)–C(9)	122.9(2)	O(4)–C(8)–C(9)	127.1(2)
O(1)–C(5)–C(6)	128.4(2)	O(4)–C(8)–C(7)	127.0(2)
C(9)–C(5)–C(6)	108.7(2)	C(9)–C(8)–C(7)	105.9(2)
O(2)–C(6)–C(5)	128.9(2)	O(5)–C(9)–C(5)	122.8(2)
O(2)–C(6)–C(7)	124.0(2)	O(5)–C(9)–C(8)	127.7(2)
C(5)–C(6)–C(7)	107.1(2)	C(5)–C(9)–C(8)	109.5(2)
O(3)–C(7)–C(6)	124.2(2)		

Symmetry transformation used to generate equivalent atoms (') $-x, 1-y, -z$.

Table 3
Selected bond lengths (Å) and angles (°) for $[Fe_2(bpym)(C_4O_4)_2(H_2O)_6]\cdot 2H_2O$ (2i)

Iron coordination sphere			
Fe–O(1)	2.052(2)	Fe–O(7)	2.156(2)
Fe–O(6)	2.104(2)	Fe–N(2)'	2.196(2)
Fe–O(5)	2.132(2)	Fe–N(1)	2.210(2)
O(1)–Fe–O(6)	93.26(8)	O(6)–Fe–N(2)'	91.29(8)
O(1)–Fe–O(5)	103.75(8)	O(5)–Fe–N(2)'	166.29(9)
O(6)–Fe–O(5)	89.89(8)	O(7)–Fe–N(2)'	92.38(8)
O(1)–Fe–O(7)	82.89(8)	O(1)–Fe–N(1)	165.08(9)
O(6)–Fe–O(7)	174.67(7)	O(6)–Fe–N(1)	88.11(8)
O(5)–Fe–O(7)	87.46(8)	O(5)–Fe–N(1)	91.11(8)
O(1)–Fe–N(2)'	89.82(8)	O(7)–Fe–N(1)	96.57(8)
Squarate group			
O(1)–C(5)	1.254(4)	C(5)–C(6)	1.453(4)
O(2)–C(6)	1.252(4)	C(5)–C(8)	1.463(4)
O(3)–C(7)	1.248(4)	C(6)–C(7)	1.475(4)
O(4)–C(8)	1.256(3)	C(7)–C(8)	1.479(4)
C(5)–O(1)–Fe	129.9(2)	O(3)–C(7)–C(6)	134.6(3)
O(1)–C(5)–C(6)	133.5(3)	O(3)–C(7)–C(8)	136.3(3)
O(1)–C(5)–C(8)	135.8(3)	C(6)–C(7)–C(8)	89.1(2)
C(6)–C(5)–C(8)	90.6(2)	O(4)–C(8)–C(5)	134.4(3)
O(2)–C(6)–C(5)	134.9(3)	O(4)–C(8)–C(7)	135.8(2)
O(2)–C(6)–C(7)	134.8(3)	C(5)–C(8)–C(7)	89.8(2)
C(5)–C(6)–C(7)	90.3(2)		

Symmetry transformation used to generate equivalent atoms (') $-x, -y, -z+1$.

Table 4
Selected bond lengths (Å) and angles (°) for $[Fe_2(bpym)(C_4O_4)_2(H_2O)_6]\cdot 2H_2O$ (2ii)

Iron coordination sphere			
Fe–O(1)	2.109(7)	Fe–O(7)	2.102(7)
Fe–O(5)	2.167(8)	Fe–N(1)	2.247(10)
Fe–O(6)	2.071(7)	Fe–N(2)'	2.196(9)
O(1)–Fe–O(5)	97.9(3)	O(5)–Fe–N(2)'	174.8(3)
O(1)–Fe–O(6)	88.2(3)	O(6)–Fe–O(7)	174.2(3)
O(1)–Fe–O(7)	93.2(3)	O(6)–Fe–N(1)	92.9(3)
O(1)–Fe–N(1)	160.8(3)	O(6)–Fe–N(2)'	89.3(3)
O(1)–Fe–N(2)'	86.7(3)	O(7)–Fe–N(1)	87.7(3)
O(5)–Fe–O(6)	88.4(3)	O(7)–Fe–N(2)'	96.4(3)
O(5)–Fe–O(7)	85.8(3)	N(1)–Fe–N(2)'	74.1(3)
O(5)–Fe–N(1)	101.3(3)		
Squarate group			
O(1)–C(5)	1.25(2)	C(5)–C(6)	1.47(2)
O(2)–C(6)	1.26(1)	C(5)–C(8)	1.46(2)
O(3)–C(7)	1.26(2)	C(6)–C(7)	1.45(2)
O(4)–C(8)	1.25(1)	C(7)–C(8)	1.46(2)
Fe–O(1)–C(5)	133.2(6)	O(3)–C(7)–C(6)	135.4(8)
O(1)–C(5)–C(6)	133.8(9)	O(3)–C(7)–C(8)	134.5(9)
O(1)–C(5)–C(8)	136.7(9)	C(6)–C(7)–C(8)	90.0(9)
C(6)–C(5)–C(8)	89(1)	O(4)–C(8)–C(5)	134(1)
O(2)–C(6)–C(5)	134(1)	O(4)–C(8)–C(7)	136(1)
O(2)–C(6)–C(7)	135(1)	C(5)–C(8)–C(7)	90.2(8)
C(5)–C(6)–C(7)	90.4(8)		

Symmetry transformation used to generate equivalent atoms (') $-x, -y, -z$.

The signals in the ^1H spectra of **1** and **2** in DMSO-d_6 solutions are broadened owing to the effect of the paramagnetic, high-spin Fe^{2+} ion. However, in each case the spectrum clearly shows the presence of two different types of protons (9.05/7.72 ppm for **1** and 8.98/7.69 ppm for **2**), the ratio between the integrals of the signals being 2:1, in accordance with the bpym bridging mode found in the crystal structures. The ^1H spectrum of compound **4** shows essentially the same features, showing that bpym bridges are also present in this compound. As the chemical analysis indicates a 2:3 Fe:bpym ratio in this compound, it is likely that there is also terminal chelating bpym and/or uncoordinated bpym present. The signals from these terminal or free bpym groups may be obscured owing to rapid exchange in solution, hence the NMR data do not exclude the simultaneous presence of bis(chelating) and chelating bpym. ^1H and ^{13}C spectra of compound **3** feature sharp peaks, showing that this is a diamagnetic, low-spin Fe(II) complex. There are three proton signals with 1:1:1 ratios between the integrals of the signals, and four different carbon signals. The spectra agree well with those reported previously for $[Fe(bpym)_3]Cl_2$, $[Fe(bpym)_3](ClO_4)_2$ and for other low-spin d^6 complexes with bpym as terminal ligand [21,31].

3.2. On the preparation of the complexes

The excess of bpym used in the syntheses of **1** and **2** protects iron(II) from being oxidized to iron(III) and prevents the precipitation of the polymeric squarato and cro-

Table 5
Hydrogen bonding for $[Fe_2(bpym)(C_5O_5)_2(H_2O)_4]\cdot 2H_2O$ (1)

Donor–H	Acceptor	D···A (Å)	H···A (Å)	D–H···A (°)
O(6)–H(61)	O(4) (−x, −y, 1−z)	2.742(3)	2.00	165
O(6)–H(62)	O(1) (−x, −y, −z)	2.820(2)	2.04	163
O(7)–H(71)	O(8) (x, y, z)	2.571(3)	1.79	175
O(7)–H(72)	O(2) (1−x, −y, −z)	2.656(3)	1.88	164
O(8)–H(81)	O(3) (x, 1+y, z)	2.949(3)	2.29	158
O(8)–H(82)	O(3) (1−x, −y, 1−z)	2.768(3)	2.00	177

Table 6
Hydrogen bonding for $[Fe_2(bpym)(C_4O_4)_2(H_2O)_6]\cdot 2H_2O$ (2i)

Donor–H	Acceptor	D···A (Å)	H···A (Å)	D–H···A (°)
O(5)–H(51)	O(3) (x, y−1, z)	2.891(3)	2.10	148
O(5)–H(52)	O(4) (x, y, z)	2.690(3)	1.93	175
O(6)–H(61)	O(4) (−x, 1−y, −z)	2.687(3)	1.87	170
O(6)–H(62)	O(8) (−x, 1−y, 1−z)	2.676(3)	1.90	170
O(7)–H(71)	O(2) (x, y−1, z)	2.630(3)	1.98	169
O(7)–H(72)	O(3) (1−x, 1−y, −z)	2.736(3)	1.79	167
O(8)–H(81)	O(2) (x, y, z)	2.740(3)	1.96	153
O(8)–H(82)	O(7) (1−x, 1−y, 1−z)	2.862(3)	1.96	156

Table 7
Possible hydrogen bonding for $[Fe_2(bpym)(C_4O_4)_2(H_2O)_6]\cdot 2H_2O$ (2ii)

Donor	Acceptor	D···A (Å)
O(5)	O(4) (x, y, z)	2.624(12)
O(5)	O(8) (1−x, −y, 1−z)	2.843(9)
O(6)	O(2) (1−x, 1−y, −z)	2.713(11)
O(6)	O(3) (x, y−1, z)	2.665(9)
O(7)	O(2) (−x, 1−y, −z)	2.689(12)
O(7)	O(8) (x−1, y, z)	2.781(9)
O(8)	O(3) (1−x, 1−y, 1−z)	2.728(11)
O(8)	O(4) (x, y, z)	2.758(11)

conato iron(II) chains; in fact, if stoichiometric ratios bpym:Fe(II) of 1:2 were used, a partially oxidized product resulted. Side products **3** and **4** with higher bpym contents were also formed in the syntheses. Mixing $FeCl_2$ and bpym in a ratio of 1:3 produced a product with IR and NMR spectra identical with **3**. The product is $[Fe(bpym)_3]Cl_2\cdot 7H_2O$ whose preparation and spectral characterization have been reported earlier [21]. Compound **4** has not been fully characterized, though solubility, chemical analysis and spectroscopic results (IR and NMR) indicate that this may be a bpym bridged dimer which also contains terminal and/or uncoordinated bpym. Compound **4** was not formed in the synthesis of the croconato compound, probably because it takes a very large excess of bpym to substitute the bidentate croconate ligand. When such a substitution is achieved, the mononuclear compound **3** is formed.

3.3. Crystal structures

3.3.1. Description of $[Fe_2(bpym)(C_5O_5)_2(H_2O)_4]\cdot 2H_2O$ (1)

The molecular unit and two waters of hydration are shown in Fig. 1. Bpym serves as a bis(chelating) bridge between

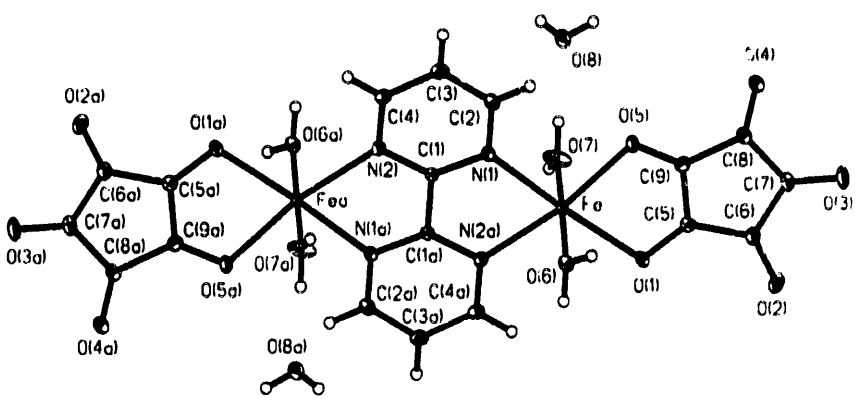

Fig. 1. The $[Fe_2(bpym)(C_5O_5)_2(H_2O)_4]\cdot 2H_2O$ (1) unit. Thermal ellipsoids are plotted at the 50% probability level. Symmetry transformation used to generate equivalent atoms (a) −x, 1−y, −z.

the two iron(II) atoms; croconate is a terminal, chelating ligand. Iron has a distorted, clearly compressed octahedral coordination geometry, with bpym nitrogen atoms (2.186(2) and 2.201(2) Å for Fe–N) and croconate oxygen atoms (2.215(2) and 2.157(2) Å for Fe–O) in the equatorial plane, and water molecules (2.025(2) and 2.084(2) Å for Fe–O) in the axial positions. The equatorial plane has a slight tetrahedral distortion, and Fe deviates only marginally, 0.022 Å, from this plane in the direction towards O(6). The dihedral angle between the equatorial plane and the bridging N_4C_2 group is 3.9°, and between the equatorial plane and the croconate ligand 5.3°. The iron–iron distance across the bpym bridge is 5.829(2) Å.

Hydrogen bonds link the molecular units in a three-dimensional network (Table 5). In particular one may notice that the coordinated water molecule O(6) of unit x, y, z is hydrogen bonded to the coordinated croconate oxygen O(1) in unit $-x, -y, -z$, creating an O(1)–Fe–O(6)–O(1)–Fe–O(6) ring where the intermolecular Fe···Fe distance is 5.335(2) Å.

3.3.2. Description of $[Fe_2(bpym)(sq)_2(H_2O)_6]\cdot 2H_2O$ (2i) and (2ii)

The molecular unit and two waters of hydration are shown for the two structures in Figs. 2 and 3. The two molecular structures are very similar. Bpym serves as a bis(chelating) bridge between metal centres, and squarate is a terminal, monodentate ligand. The iron atom in each case has a distorted, octahedral geometry, with bpym nitrogen atoms (2.210(2), 2.196(2) Å (**2i**) and 2.247(10), 2.196(9) Å (**2ii**) for Fe–N), squarate oxygen (2.052(2) (**2i**) and 2.109(7) Å (**2ii**) for Fe–O(1)) and a water molecule (2.132(2) (**2i**) and 2.167(7) Å (**2ii**) for Fe–O(5)) in equatorial positions, and water molecules in axial positions (2.104(2), 2.156(2) Å (**2i**) and 2.071(7), 2.102(7) Å (**2ii**) for Fe–O). The equatorial plane in **2i** does not deviate significantly from planarity, while the plane in **2ii** has a slight tetrahedral distortion; the iron atoms deviate by 0.028 and 0.015 Å, respectively, from these planes. The dihedral angles of the equatorial plane/bridging N_4C_2 group and equatorial plane/squarato ligand are 2.3 and 19.2° for **2i**, 1.9 and 6.8° for **2ii**. In each case there is an intramolecular hydrogen bond between the equatorial water molecule O(5) and an uncoordinated squarate oxygen, O(4). The iron–iron distance across the bpym bridge is 5.869(1) in **2i** and 5.941(3) Å in **2ii**, the longer distance in the latter complex being reflected in a longer Fe–N(1) bond and a smaller N–Fe–N angle.

The main differences in the two structures are found in the packing and hydrogen bond pattern. As shown by the densi-

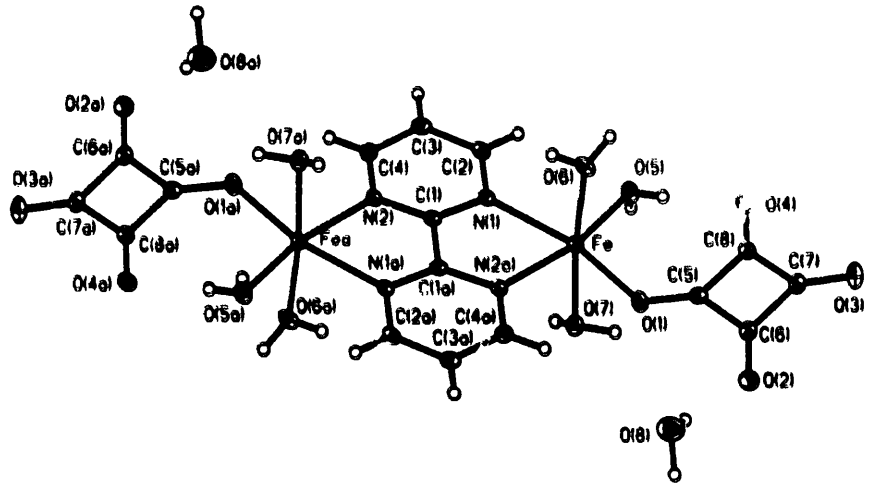

Fig. 2. The $[Fe_2(bpym)(C_4O_4)_2(H_2O)_6]\cdot 2H_2O$ (**2i**) unit. Thermal ellipsoids are plotted at the 50% probability level. Symmetry transformation used to generate equivalent atoms (a) $-x, -y, 1-z$.

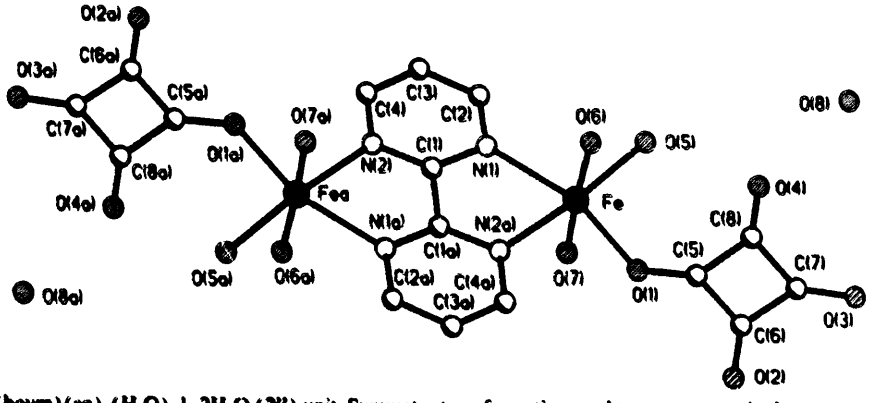

Fig. 3. The $[Fe_2(bpym)(sq)_2(H_2O)_6]\cdot 2H_2O$ (**2ii**) unit. Symmetry transformation used to generate equivalent atoms (a) $-x, -y, -z$.

Table 8
Selected magnetostructural data for bpym-bridged iron(II) and copper(II) complexes

Compound	Nuclearity	M–N(bpym) [a] (Å)	M···M [b] (Å)	$-J$ [c] (cm^{-1})	$n_A n_B J$	Ref.
$[Fe_2(bpym)_3(NCS)_4]$	dimer	2.27	6.050(6)	4.1	65.6	[32]
$[Fe_2(bpym)(H_2O)_8](SO_4)_2 \cdot 2H_2O$	dimer	2.22	5.836(1)	3.4	54.4	[33]
$[Fe_2(bpym)(H_2O)_6(SO_4)_2]$	dimer	2.22	5.909(1)	3.1	49.6	[33]
$[Fe(bpym)(NCS)_2]_n$	chain	2.24	5.960(1)	3.5	56	[34]
1	dimer	2.19	5.829(2)	3.7	59.2	this work
2i	dimer	2.20	5.869(1)	5.9	94.4	this work
$[Cu_2(bpym)(C_5O_5)_2(H_2O)_2] \cdot 2H_2O$	dimer	2.02	5.384(1)	160	160	[17f]
$[Cu_2(bpym)(C_4O_4)_2(H_2O)_6]$	dimer	2.07	5.542(1)	139	139	[12h]

[a] Average value for the metal-to-nitrogen (bridging bpym) bond.
[b] Metal–metal separation across bpym.
[c] Exchange interaction through bridging bpym.

ties of the two polymorphs (Table 1), **2i** has a slightly more dense packing than **2ii**. Despite this, the shortest intermolecular Fe···Fe distance in **2i**, 6.624(2) Å, is appreciably longer than the shortest Fe···Fe distance in **2ii**, 5.582(2) Å. In **2ii** the molecules are stacked such that the squarate ring of the reference molecule overlaps with the pyridyl ring of a symmetry related molecule, the closest approach being O(2)···C(1)$(x,1+y,z)$ = 3.07 Å.

3.3.3. Comparison of bpym-bridged Fe(II) compounds

To our knowledge the structures of three other Fe(II) bpym bridged dinuclear complexes and one chain compound have been reported, $[Fe_2(bpym)(NCS)_4(bpym)_2]$ [32], $[Fe_2(H_2O)_8(bpym)](SO_4)_2 \cdot 2H_2O$ [33], $[Fe_2(H_2O)_6(bpym)(SO_4)_2]$ [33], and $[Fe(bpym)(NCS)_2]_n$ [34]. The results of the present structures compare well with those previously reported (see Table 8). The Fe–N(bpym) distances range from 2.186(2) to 2.316(6) Å in the seven known structures; both close to equal and clearly unequal Fe–N(chelate) distances have been encountered. The intramolecular Fe···Fe distance across the bpym-bridge varies from 5.829(2) Å (**1**) to 6.050(6) Å (note that the latter distance is given erroneously as 5.522(6) Å in Ref. [32]). In all of the dimeric structures the dihedral angle between the Fe equatorial plane and the bridging unit is small, ranging from 2.4° to 10.9° [33].

3.4. Magnetic properties

The magnetic properties of complexes **1** and **2i** in the form of plots of both χ_M (molar magnetic susceptibility) and $\chi_M T$ versus T are depicted in Figs. 4 and 5. Both curves are quite similar and they are characteristic of an antiferromagnetic interaction between the two high-spin iron(II) ions, with a molecular spin singlet ground state: the susceptibility curves show maxima at 11.5 (**1**) and 18.5 K (**2i**) whereas those of $\chi_M T$ exhibit a rapid decrease in the low temperature region, with $\chi_M T = 7.01$ (**1**) and 7.25 $cm^3\ mol^{-1}\ K$ (**2i**) at 290 K (the calculated value for a pair of magnetically isolated high-spin iron(II) ions is 7.26 $cm^3\ mol^{-1}\ K$ with $g = 2.20$) and an extrapolated value that vanishes when T approaches zero. All our attempts to analyse the susceptibility data of **1** and **2i** in terms of an isotropic exchange interaction model for a dinuclear species (the Hamiltonian being $H = -JS_A \cdot S_B$ with $S_A = S_B = 2$) failed. The consideration of intermolecular interactions did not improve significantly the quality of the fit. Most likely, the orbital contribution associated with a six coordinate iron(II) ion accounts for this mismatch between the computed and experimental data. Although the metal surroundings in **1** and **2i** exhibit a significant distortion from

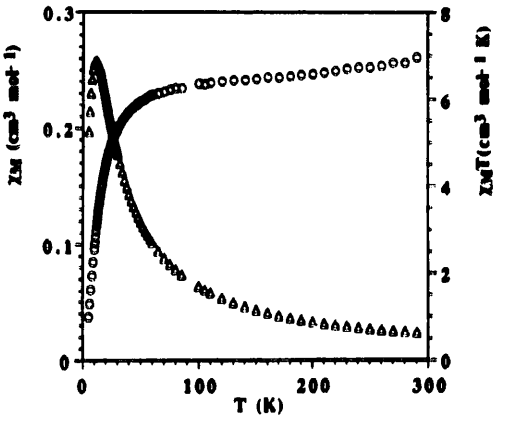

Fig. 4. Temperature dependence of χ_M (Δ) and $\chi_M T$ (○) for complex **1**.

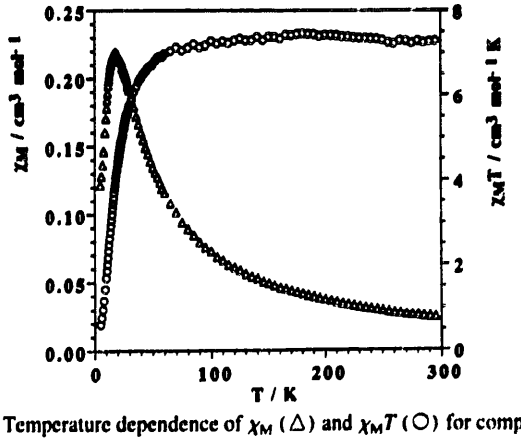

Fig. 5. Temperature dependence of χ_M (Δ) and $\chi_M T$ (○) for complex **2i**.

an ideal octahedron, this lowering of symmetry evidently is not sufficient to reduce the orbital contribution to a negligible level. Anyway, taking into account the ratio which relates the value of the exchange parameter and the temperature T_{max} for which a maximum of susceptibility is observed ($|J|/kT_{max}=0.462$ for two interacting $S=2$ local spins) [35], values of $J=-3.7$ (**1**) and $-5.9\,cm^{-1}$ (**2i**) are easily found.

Selected magnetostructural data dealing with bpym-bridged iron(II) complexes are listed in Table 8. Related copper(II) complexes are included for the sake of comparison. The value of the magnetic coupling for complex **1** lies within the range of the previously reported values, whereas that of complex **2i** is larger. This latter value is most likely overestimated because it includes factors such as the zero-field splitting which can be very important for high-spin iron(II) [36]. The exchange pathway accounting for the significant antiferromagnetic coupling which is observed in the bpym-bridged metal complexes is the σ in-plane overlap between the $d_{x^2-y^2}$ type magnetic orbitals of each metal ion (the x and y axes being defined by the M–N(bridging bpym) bonds) which we have discussed elsewhere [37]. In the case of Cu(II) (only one unpaired electron per metal ion and located in a $d_{x^2-y^2}$ type magnetic orbital), the σ exchange pathway is the only one which is operative, whereas in the case of Fe(II) (four unpaired electrons per metal ion), the π exchange pathway also participates. However, the appreciable lowering of the value of $-J$ when going from Cu(II) to Fe(II) indicates that the π contribution must be negligible. A more appropriate analysis of this variation requires taking into account that the experimental J parameter can be decomposed into a sum of individual contributions, $J_{\mu\nu}$, involved in the exchange phenomenon [38]:

$$J=1/n_A n_B \sum_{\mu=1}^{n_A}\sum_{\nu=1}^{n_B} J_{\mu\nu} \qquad (1)$$

where n_A and n_B are the number of unpaired electrons on the metal ions A and B. The magnitude of the net antiferromagnetic interaction is thus properly described by $n_A n_B J$ and not by J. This value is much larger for the Cu(II) family than for the Fe(II) series (Table 8). The occurrence of ferromagnetic terms $J_{\mu\nu}$ in Eq. (1) for the Fe(II) family cannot account for this trend because they are certainly negligible at distances between magnetic centres as large as 5 Å [39]. Consequently, Eq. (1) is reduced to

$$n_A n_B J \approx J_{x^2-y^2,x^2-y^2} \qquad (2)$$

Taking into account that the energy of the $3d_{x^2-y^2}$ orbitals for Cu(II) is closer to that of the symmetry-adapted HOMOs of bpym, a larger overlap between the magnetic orbitals through bridging bpym is predicted in the case of Cu(II) versus Fe(II), and consequently a greater $-J_{x^2-y^2,x^2-y^2}$ value. This explains satisfactorily the different values of the magnetic coupling shown in Table 8.

3.5. Complexity of the Fe(II):bpym system

We would like to finish the present contribution with some comments about the different nuclearity and spin states that can be obtained in the Fe(II):bpym system by using as tools the Fe(II) to bpym molar ratio and either coordinating counterions or coligands in aqueous solution. The reaction of iron(II) and bpym in a 1:3 metal to ligand molar ratio yields the low-spin species $[Fe(bpym)_3]^{2+}$ which has been isolated either as a chloride [21] or as a perchlorate salt [22]. Bpym has an equally strong ligand field character versus Fe(II) as 2,2′-bipyridine (bpy) and 1,10-phenanthroline (phen). The advantage of the tris(bpym)iron(II) complex over the related bpy or phen species lies in the possibility of using it as a stable tris(chelating) ligand to prepare polymetallic species. When the metal to bpym molar ratio is decreased, the centrosymmetric dinuclear $[Fe_2(bpym)_3(NCS)_4]$ [32] and the chiral $[Fe(bpym)(NCS)_2]_n$ chain [34] compounds, with coordinating thiocyanate ligands in *cis* positions, were obtained. The compounds are both high-spin species with a significant antiferromagnetic coupling. Although the metal environment in both compounds is typical of spin crossover [40,41], they do not exhibit any spin transition. Finally, for the highest metal to bpym molar ratio used, Fe(II):bpym 2:1, the dinuclear $[Fe_2(bpym)(H_2O)_8](SO_4)_2\cdot 2H_2O$ and $[Fe_2(bpym)(H_2O)_6(SO_4)_2]$ complexes [33] were isolated in the presence of a poorly coordinating anion such as sulfate. The use of the dinegative croconate and squarate ligands yields the insoluble dinuclear complexes **1** and **2** which are the subject of the present work. The insolubility of these species in water apparently precludes the formation of higher dimensionality compounds through bridging croconate or squarate. However, the prospect of obtaining higher dimensionality compounds with the iron(II):bpym:croconate/squarate systems is not hopeless. In this context it deserves to be noted that the formation of the neutral sheetlike polymers of formula $[Fe_2(bpym)(N_3)_4]$ [42] and $[Fe_2(bpym)(ox)_2]\cdot 5H_2O$ [43] (N_3^- and ox are azide and oxalate respectively) has been observed, where $[Fe_2(bpym)]^{4+}$ units are polymerized through bis-chelating oxalate or double end-on azido groups.

4. Supplementary material

Fractional coordinates for all atoms and anisotropic displacement parameters have been deposited at the Cambridge Crystallographic Data Centre, 12 Union Road, Cambridge CB2 1EZ, UK.

Acknowledgements

Financial support from the Spanish DGICYT, Project PB94-1002 (F.L. and M.J.) is gratefully acknowledged.

References

[1] L. Gmelin, Ann. Phys. (Leipzig) 4 (1825) 31.
[2] S. Cohen, J.R. Lacher, J.D. Park, J. Am. Chem. Soc. 31 (1959) 3480.
[3] (a) J.C. Trombe, J.F. Petit, A. Gleizes, New J. Chem. 12 (1988) 197; (b) J.F. Petit, A. Gleizes, J.C. Trombe, Inorg. Chim. Acta 167 (1990) 51; (c) J.C. Trombe, J.F. Petit, A. Gleizes, Inorg. Chim. Acta 167 (1990) 69; (d) J.C. Trombe, J.F. Petit, A. Gleizes, Eur. J. Solid State Inorg. Chem. 28 (1991) 669 (e) A. Bouayad, C. Brouca-Cabarrecq, J.C. Trombe, A. Gleizes, Inorg. Chim. Acta 195 (1992) 193.
[4] (a) O. Simonsen, H. Toftlund, Inorg. Chem. 20 (1981) 4044; (b) G. Bernardelli, P. Castan, R. Soules, Inorg. Chim. Acta 120 (1986) 205; (c) P. Castan, D. Deguenon, P.L. Fabre, Polyhedron 11 (1992) 901.
[5] (a) Q. Chen, L. Ma, S. Liu, J. Zubieta, J. Am. Chem. Soc. 111 (1989) 5944; (b) Q. Chen, S. Liu, J. Zubieta, Inorg. Chim. Acta 164 (1989) 115; (c) Q. Chen, S. Liu, J. Zubieta, Angew. Chem., Int. Ed. Engl. 29 (1990) 70.
[6] C. Robl, A. Weiss, Z. Anorg. Allg. Chem. 546 (1987) 161.
[7] (a) C. Robl, V. Gnutzmann, A. Weiss, Z. Anorg. Allg. Chem. 549 (1987) 187; (b) C. Robl, A. Weiss, Mater. Res. Bull. 22 (1987) 373.
[8] M.I. Khan, Y.D. Chang, Q. Chen, J. Salta, Y.S. Lee, C.J. O'Connor, J. Zubieta, Inorg. Chem. 33 (1994) 6340.
[9] (a) V.P. Chesisek, F. Doany, Acta Crystallogr., Sect. B 37 (1981) 1076; (b) E. Bang, K. Michelsen, K.M. Nielsen, E. Pedersen, Acta Chem. Scand. 43 (1989) 748.
[10] (a) F. Lloret, M. Julve, J. Faus, X. Solans, Y. Journaux, I. Morgenstern-Badarau, Inorg. Chem. 29 (1990) 2232; (b) G.M. Frankenbach, M.A. Beno, A.M. Kini, J.M. Williams, U. Welp, J.E. Thompson, Inorg. Chim. Acta 192 (1992) 195.
[11] (a) M. Habenschuss, B.C. Gerstein, Chem. Phys. 61 (1974) 852; (b) J.A.C. van Ooijen, J. Reedijk, A.L. Spek, Inorg. Chem. 18 (1979) 1184; (c) A. Weiss, E. Riegler, C. Robl, Z. Naturforsch., Teil B 41 (1986) 1329; (d) R. Soules, F. Dahan, J.P. Laurent, P. Castan, J. Chem. Soc., Dalton Trans. (1988) 587; (e) I. Castro, M.L. Calatayud, J. Sletten, F. Lloret, M. Julve, J. Chem. Soc., Dalton Trans. (1997) 811.
[12] (a) C. Robl, A. Weiss, Z. Naturforsch., Teil B 41 (1986) 1311; (b) G. Bernardelli, D. Deguenon, R. Soules, P. Castan, Can. J. Chem. 67 (1989) 1158; (c) X. Solans, M. Aguiló, A. Gleizes, J. Faus, M. Julve, M. Verdaguer, Inorg. Chem. 29 (1990) 775; (d) M. Beneto, L. Soto, J. García Lozano, E. Escrivá, J.P. Legros, F. Dahan, J. Chem. Soc., Dalton Trans. (1991) 1057; (e) I. Castro, J. Faus, M. Julve, Y. Journaux, J. Sletten, J. Chem. Soc., Dalton Trans. (1991) 2533; (f) C.E. Xanthopoulos, M.P. Sigalas, G.A. Katsoulos, C.A. Tsipis, C.C. Hadjikostas, A. Terzis, M. Mentzafos, Inorg. Chem. 32 (1993) 3743; (g) I. Castro, J. Sletten, M.L. Calatayud, M. Julve, J. Cano, F. Lloret, A. Caneschi, Inorg. Chem. 34 (1995) 4903; (h) I. Castro, J. Sletten, L.K. Glærum, J. Cano, F. Lloret, J. Faus, M. Julve, J. Chem. Soc., Dalton Trans. (1995) 3207.
[13] (a) J.C. Trombe, C. Brouca-Cabarrecq, C.R. Acad. Sci. 310 (II) (1990) 521; (b) C. Brouca-Cabarrecq, J.C. Trombe, C.R. Acad. Sci. 311 (II) (1990) 1179; C. Brouca-Cabarrecq, J.C. Trombe, Inorg. Chim. Acta 191 (1992) 227; 191 (1992) 241.
[14] Q. Chen, S. Liu, J. Zubieta, Inorg. Chim. Acta 175 (1990) 241.
[15] (a) M.D. Glick, L.F. Dahl, Inorg. Chem. 5 (1966) 289; (b) D. Deguenon, G. Bernardelli, J.P. Tuchagues, P. Castan, Inorg. Chem. 29 (1990) 3031; (c) A. Cornia, A.C. Fabretti, A. Giusti, F. Ferraro, D. Gatteschi, Inorg. Chim. Acta 212 (1993) 87.
[16] D. Deguenon, P. Castan, F. Dahan, Acta Crystallogr., Sect. C 47 (191) 433.
[17] (a) M.D. Glick, G.L. Downs, L.F. Dahl, Inorg. Chem. 3 (1964) 1712; (b) P. Castan, D. Deguenon, F. Dahan, Acta Crystallogr., Sect. C 47 (1991) 2656; (c) I. Castro, J. Sletten, J. Faus, M. Julve, J. Chem. Soc., Dalton Trans. (1992) 2271; (d) M. Aguiló, X. Solans, I. Castro, J. Faus, M. Julve, Acta Crystallogr., Sect. C 48 (1992) 2; (e) I. Castro, J. Sletten, J. Faus, M. Julve, Y. Journaux, F. Lloret, S. Alvarez, Inorg. Chem. 31 (1992) 1889; (f) I. Castro, J. Sletten, L.K. Glærum, F. Lloret, J. Faus, M. Julve, J. Chem. Soc., Dalton Trans. (1994) 2777; (g) G. Speier, E. Speier, B. Noll, C.G. Pierpont, Inorg. Chem. 36 (1997) 1520.
[18] F. Serratosa, Acc. Chem. Res. 16 (1983) 170.
[19] K. Yamada, Y. Hirata, Bull. Chem. Soc. Jpn. 31 (1958) 550.
[20] K. Schwartz, R.I. Gelb, J.O. Yardley, J. Phys. Chem. 79 (1975) 2246.
[21] R.D. Gillard, R.J. Lancashire, P.A. Williams, Transition Met. Chem. 4 (1979) 115.
[22] G. De Munno, M. Julve, J.A. Real, Inorg. Chim. Acta 255 (1997) 185.
[23] (a) A.C.T. North, D.C. Phillips, F.S. Mathews, Acta Crystallogr., Sect. A 24 (1968) 351; (b) G. Kopfman, R. Huber, Acta Crystallogr., Sect. A 24 (1968) 348.
[24] N. Walker, D. Stuart, Acta Crystallogr., Sect. A 39 (1983) 159.
[25] (a) R.H. Blessing, J. Appl. Crystallogr. 22 (1989) 396; (b) R.H. Blessing, Cryst. Rev. 1 (1987) 3.
[26] (a) G.M. Sheldrick, Acta Crystallogr., Sect. A 46 (1990) 467; (b) G.M. Sheldrick, SHELXL-93, University of Göttingen, Germany, 1993; (c) G.M. Sheldrick, SHELXTL-PLUS Version 4.21, Siemens Analytical X-Ray Instruments, Inc., Madison, WI, 1990.
[27] MolEN, an interactive structure solution procedure, Enraf-Nonius, Delft, Netherlands, 1990.
[28] M. Ito, R. West, J. Am. Chem. Soc. 85 (1963) 2580.
[29] (a) J.T. Reinprecht, J.G. Miller, G.C. Vogel, M.S. Haddad, D.N. Hendrickson, Inorg. Chem. 19 (1980) 927; (b) C.G. Pierpont, L.C. Francesconi, D.N. Hendrickson, Inorg. Chem. 17 (1978) 3470; (c) F.G. Baglin, C.B. Rose, Spectrochim. Acta A. 26 (1970) 2293; (d) R. West, Y.H. Niu, J. Am. Chem. Soc. 85 (1963) 2586.
[30] M. Julve, M. Verdaguer, G. De Munno, J.A. Real, G. Bruno, Inorg. Chem. 32 (1993) 795.
[31] (a) R.R. Ruminski, K.D. Van Tassel, J.D. Petersen, Inorg. Chem. 23 (1984) 4380; (b) C. Overton, J.A. Connor, Polyhedron 1 (1982) 53.
[32] J.A. Real, J. Zarembowitch, O. Kahn, X. Solans, Inorg. Chem. 26 (1987) 2939.
[33] E. Andrés, G. De Munno, M. Julve, J.A. Real, F. Lloret, J. Chem. Soc., Dalton Trans. (1993) 2169.
[34] G. De Munno, M. Julve, J.A. Real, F. Lloret, R. Scopelliti, Inorg. Chim. Acta 250 (1996) 81.
[35] O. Kahn, Molecular Magnetism, VCH, New York, 1993, p. 112.
[36] R.L. Carlin, Magnetochemistry, Springer, Berlin, 1986.
[37] M. Julve, G. De Munno, G. Bruno, M. Verdaguer, Inorg. Chem. 27 (1988) 3160.
[38] O. Kahn, Struct. Bonding (Berlin) 68 (1987) 89 and Refs. therein.
[39] P. Román, C. Guzmán-Miralles, A. Luque, J.I. Beitia, J. Cano, F. Lloret, M. Julve, S. Alvarez, Inorg. Chem. 35 (1996) 3741.
[40] M. Konno, M. Mikami-Kido, Bull. Chem. Soc. Jpn. 64 (1991) 339.
[41] T. Granier, B. Gallois, J. Gaultier, J.A. Real, J. Zarembowitch, Inorg. Chem. 32 (1993) 5305.
[42] G. De Munno, T. Poerio, G. Viau, M. Julve, F. Lloret, Y. Journaux, E. Rivière, Chem. Commun. (1996) 2587.
[43] G. De Munno, M. Julve, F. Lloret, in preparation.